

# An Integrated Bioinformatics Approach for Identifying Genetic Markers that Predict Cerebrospinal Fluid Biomarker p-tau<sub>181</sub>/Aβ<sub>1-42</sub> Ratio in APOE4-Negative Mild Cognitive Impairment Patients

Ying Sun<sup>a,b,\*</sup>, Anders Bresell<sup>c</sup>, Mattias Rantalainen<sup>d</sup>, Kina Höglund<sup>a,e</sup>, Thibaud Lebouvier<sup>f</sup>, Hugh Salter<sup>a,b</sup> and the Alzheimer Disease Neuroimaging Initiative<sup>1</sup>

<sup>a</sup>AstraZeneca Translational Science Centre, Personalised Healthcare & Biomarkers, Innovative Medicines, AstraZeneca R&D, Sweden

<sup>b</sup>Department Clinical Neuroscience, Science for Life Laboratory, Karolinska Institutet, Solna, Sweden

<sup>c</sup>Clinical Informatics, CNS/Pain Clinical Development, AstraZeneca R&D Södertälje, Sweden

<sup>d</sup>Department of Medical Epidemiology and Biostatistics, Karolinska Institutet, Sweden

<sup>e</sup>Institute of Neuroscience & Physiology, Department of Psychiatry & Neurochemistry, The Sahlgrenska Academy at University of Gothenburg, Sweden

<sup>f</sup>Department of Immunology, Genetics and Pathology, Uppsala University, Sweden

Handling Associate Editor: Henrik Zetterberg

Accepted 12 January 2015

**Abstract.** Alzheimer's disease (AD) is the most common form of dementia, with no disease-modifying treatment yet available. Early detection of patients at risk of developing AD is of central importance. Blood-based genetic signatures can serve as early detection and as population-based screening tools. In this study, we aimed to identify genetic markers and gene signatures associated with cerebrospinal fluid (CSF) biomarkers levels of t-tau, p-tau<sub>181</sub>, and with the two ratios t-tau/Aβ<sub>1-42</sub> and p-tau<sub>181</sub>/Aβ<sub>1-42</sub> in the context of progression from mild cognitive impairment (MCI) to AD, and to identify a panel of genetic markers that can predict CSF biomarker p-tau<sub>181</sub>/Aβ<sub>1-42</sub> ratio with consideration of APOE4 stratification. We analyzed genome-wide the Alzheimer's Disease Neuroimaging Initiative dataset with up to 48 months follow-up. In the first part of the analysis, the main effect of single nucleotide polymorphisms (SNPs) under an additive genetic model was assessed for each of the four CSF biomarkers. In the second part of the analysis, we performed an integrated analysis of genome-wide association study results with pathway enrichment analysis, predictive modeling and network analysis in the subgroup of APOE4-negative subjects. We identified a panel of five SNPs, rs6766238, rs1143960, rs1249963, rs11975968, and rs4836493, that are predictive for

<sup>1</sup>Data used in preparation of this article were obtained from the Alzheimer's Disease Neuroimaging Initiative (ADNI) database (<http://adni.loni.usc.edu>). As such, the investigators within the ADNI contributed to the design and implementation of ADNI and/or provided data but did not participate in analysis or writing of this report. A complete listing of ADNI investigators can be found at: [http://adni.loni.usc.edu/wpcontent/uploads/how\\_to\\_apply/ADNI\\_](http://adni.loni.usc.edu/wpcontent/uploads/how_to_apply/ADNI_)

Acknowledgement.List.pdf

\*Correspondence to: Ying Sun, AstraZeneca Translational Science Centre, Personalised Healthcare & Biomarkers, Innovative Medicines, AstraZeneca R&D, Science for Life Laboratory, Tomtebodavägen 23A, SE-171 65, Solna, Sweden. Tel.: +46 8 55329330; Fax: +46 8 524 81425; E-mail: Ying.Sun2015@gmail.com.

28 p-tau<sub>181</sub>/A $\beta$ <sub>1-42</sub> ratio (high/low) with a sensitivity of 66% and a specificity of 70% (AUC 0.74). These results suggest that a  
29 panel of SNPs is a potential prognostic biomarker in APOE4-negative MCI patients.

30 Keywords: Alzheimer's disease, cerebrospinal fluid, genome-wide association study, mild cognitive impairment, multivariate  
31 analysis, pathway analysis, predictive model

## 28 INTRODUCTION

29 Alzheimer's disease (AD) is the most common form  
30 of dementia, with no disease-modifying treatment yet  
31 available. It has been estimated that 35.6 million peo-  
32 ple lived with dementia worldwide in 2010 and that AD  
33 accounts for about 60–80% of these cases [1]. Patients  
34 with amnesic mild cognitive impairment (aMCI) have  
35 mild but measurable changes in cognitive abilities,  
36 especially executive memory, which is considered a  
37 prodromal stage of AD [2] when supported by the  
38 presence of abnormal biomarkers. The rate of progres-  
39 sion from aMCI to AD is up to 10% per year [3]. In  
40 an aging society, early detection as well as early ther-  
41 apy is widely considered to be an important goal for  
42 researchers. Therefore, aMCI is an important clinical  
43 group in which to study longitudinal changes associ-  
44 ated with the development of AD.

45 The emerging criteria for diagnosis of AD require  
46 the presence of an appropriate clinical AD pheno-  
47 type together with one or more pathophysiological  
48 biomarker(s) consistent with the presence of AD  
49 pathology [4–6]. Biomarkers that can be utilized as  
50 surrogate markers of underlying pathological change  
51 have become of central importance for detection of  
52 early and preclinical AD. Efforts have been made  
53 by researchers worldwide to identify and validate  
54 different biomarkers for the early diagnosis and/or pre-  
55 diction of progression from MCI to AD, including  
56 positron emission tomography (PET) imaging lig-  
57 ands, archetypically Pittsburgh compound B (PiB),  
58 which bind to amyloid- $\beta$  (A $\beta$ ), PET imaging with  
59 <sup>18</sup>F-FDG to measure local glucose metabolism [7–10],  
60 structural magnetic resonance imaging (MRI) and  
61 cerebrospinal fluid (CSF) biochemical biomarkers,  
62 especially A $\beta$ <sub>1-42</sub>, total tau (t-tau), and tau phospho-  
63 rylated at threonine 181 (p-tau<sub>181</sub>) either alone, or  
64 in combination with imaging and CSF biomarkers  
65 [11–14]. It has been reported that the combination  
66 of increased CSF concentrations of t-tau or p-tau<sub>181</sub>  
67 and decreased concentration of A $\beta$ <sub>1-42</sub> improves sen-  
68 sitivity and specificity in the diagnosis of AD, and  
69 that these markers are predictive of future conver-  
70 sion from MCI to AD [15–18]. However, both PET

71 imaging and CSF biomarkers have only had limited use  
72 in population-based screening, because they are inva-  
73 sive and relatively expensive. Therefore, blood-based  
74 biomarkers are needed to develop more affordable  
75 and more widely accessible diagnostic and prognostic  
76 tests.

77 Genetic markers may facilitate improved methods  
78 for early detection and for patient segmentation, as well  
79 as illuminating potential therapeutic avenues. Muta-  
80 tions have been identified in genes that encode the  
81 amyloid precursor protein (*APP*), presenilin-1 (*PS1*),  
82 and presenilin-2 (*PS2*) in familial AD [19]. In sporadic  
83 late-onset AD (LOAD), presence of alleles encoding  
84 the apolipoprotein E4 isoform (APOE4) is a strong  
85 risk factor associated with AD [20, 21]. Recently,  
86 genome-wide association studies (GWAS) have iden-  
87 tified common variants in genes *PLD3*, *CD2AP*, *CD33*,  
88 *MS4A/MS4A6E*, and *EPHA1* as novel candidates asso-  
89 ciated with LOAD diagnosis [22, 23] and other GWASs  
90 have identified variants in *PPP3R1* and *MAPT* as asso-  
91 ciated with progression of AD [24]. However, genetic  
92 variants discovered by single-locus based GWAS typi-  
93 cally identified variants with small effects sizes in their  
94 association with the phenotype, here AD or AD pro-  
95 gression, and therefore the individual SNPs do not  
96 by themselves constitute potent biomarkers for dis-  
97 ease diagnosis and monitoring of AD progression.  
98 Multivariate panels of genetic variants may, however,  
99 provide more powerful means for diagnostic and prog-  
100 nostic applications. To the best of our knowledge,  
101 no studies to date have reported multivariate pan-  
102 els of SNPs for prediction of progression from MCI  
103 to AD. Moreover, there is relatively little knowledge  
104 about diagnostic accuracy and marker selection in  
105 APOE4-negative patients specifically. A recent study  
106 reported that use of CSF biomarkers as a predictor  
107 of conversion from MCI to AD performed better in  
108 APOE4-negative subjects than APOE4-positive sub-  
109 jects [25]. To address these questions, we conducted  
110 an integrated analytic approach to search for predic-  
111 tive genetic markers as surrogate markers of CSF  
112 biomarkers aimed at improving the possibility to pre-  
113 dict progression from MCI to AD alongside APOE4  
114 status.

115 In our present study, our strategy was to identify  
 116 significant pathway-related SNPs derived from GWAS  
 117 findings, and to construct a multivariate predictive  
 118 model with selected pathway-related SNPs. We ini-  
 119 tially applied a GWAS approach to identify common  
 120 genetic polymorphisms with the strongest associa-  
 121 tion with each one of four quantitative traits, t-tau,  
 122 p-tau<sub>181</sub> levels, and the two ratios t-tau/Aβ<sub>1-42</sub> and  
 123 p-tau<sub>181</sub>/Aβ<sub>1-42</sub>, representing progression/conversion  
 124 from MCI to AD. Due to limited statistical power as  
 125 well as limitation of a single-locus analysis approach  
 126 which may lead to false negatives in respect to SNPs  
 127 contributing to joint genetic effects, we performed  
 128 pathway enrichment analysis to select significant  
 129 pathway-related genes/SNPs. Finally, we applied Ran-  
 130 dom Forest (RF) [26], a machine learning method, to  
 131 determine a candidate panel of five SNPs with the abil-  
 132 ity to predict p-tau<sub>181</sub>/Aβ<sub>1-42</sub> ratio level (high/low) in  
 133 APOE4-negative subjects.

## 134 MATERIAL AND METHODS

### 135 ADNI

136 Data used in the preparation of this article were  
 137 obtained from the Alzheimer's Disease Neuroimaging  
 138 Initiative (ADNI) database (<http://adni.loni.usc.edu>).  
 139 ADNI study was launched in 2004 by the National  
 140 Institute on Aging (NIA), the National Institute of  
 141 Biomedical Imaging and Bioengineering (NIBIB), the  
 142 Food and Drug Administration (FDA), private phar-  
 143 maceutical companies and non-profit organizations,  
 144 as a \$60 million, 5-year public-private partnership.  
 145 The primary goal of ADNI has been to test whether  
 146 serial MRI, PET, other biological markers, and clinical  
 147 and neuropsychological assessment can be combined  
 148 to measure the progression of MCI and early AD.  
 149 Determination of sensitivity and specificity of mark-  
 150 ers of very early AD progression is intended to aid  
 151 researchers and clinicians to develop new treatments  
 152 and monitor their effectiveness, as well as lessen the  
 153 time and cost of clinical trials. The initial goal of ADNI  
 154 (ADNI1) was to recruit 800 subjects from over 50 sites  
 155 across the U.S. and Canada.

### 156 Samples and genotyping

157 Genotype data of the subjects in ADNI cohort,  
 158 who meet entry criteria for the clinical diag-  
 159 nosis of normal cognition, amnesic MCI or  
 160 probable AD were downloaded from the LONI  
 161 website ([http://adni.loni.usc.edu/data-samples/access-](http://adni.loni.usc.edu/data-samples/access-data/)  
 162 [data/](http://adni.loni.usc.edu/data-samples/access-data/)). Population stratification was observed on

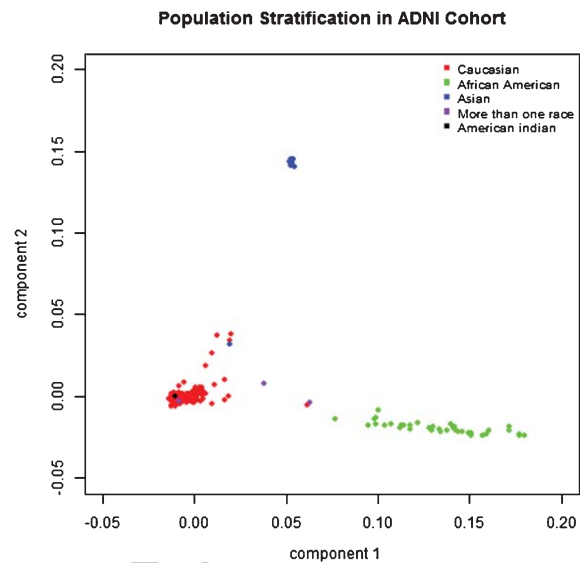


Fig. 1. Multidimensional scaling plot subjects in ADNI. Each dot represents a subject and the distance between dots represents overall genetic similarity calculated using whole genome SNP data. Majority of subjects are self-declared Caucasian (red color), the second large group is African American (green), and third large group is Asian (blue).

163 multidimensional scaling plots of the genome-  
 164 wide identity-by-state (IBS) pairwise distance matrix  
 165 (Fig. 1), therefore, only Caucasian subjects were  
 166 included in further analysis. A total of 177 MCI sub-  
 167 jects with 48 months follow-up and available CSF  
 168 biomarkers data for Aβ<sub>1-42</sub>, p-tau<sub>181</sub> and t-tau at base-  
 169 line were analyzed. Subjects were defined as MCI to  
 170 AD converter (MCI-con) if they converted from MCI  
 171 to AD at any time within 48 months and the remainder  
 172 defined as MCI stable (MCI-stable).

173 Since in this longitudinal study the baseline sam-  
 174 ples from the same subject were analyzed in different  
 175 visiting times with other samples from later visits, we  
 176 estimated and adjusted for any batch effect in the base-  
 177 line CSF values using a linear model in which batch  
 178 was included as an adjustment variable. Genotyping  
 179 data from the Human610-Quad BeadChip (Illumina,  
 180 Inc., San Diego, CA) included 620,901 SNP and copy  
 181 number variation (CNV) markers and was completed  
 182 on all ADNI subjects using the protocol as described  
 183 previously [27]. All samples also had an APOE geno-  
 184 type available in the ADNI database.

### 185 Quality control (QC)

186 The following QC procedures were implemented  
 187 prior to GWAS analysis. SNPs and individuals were

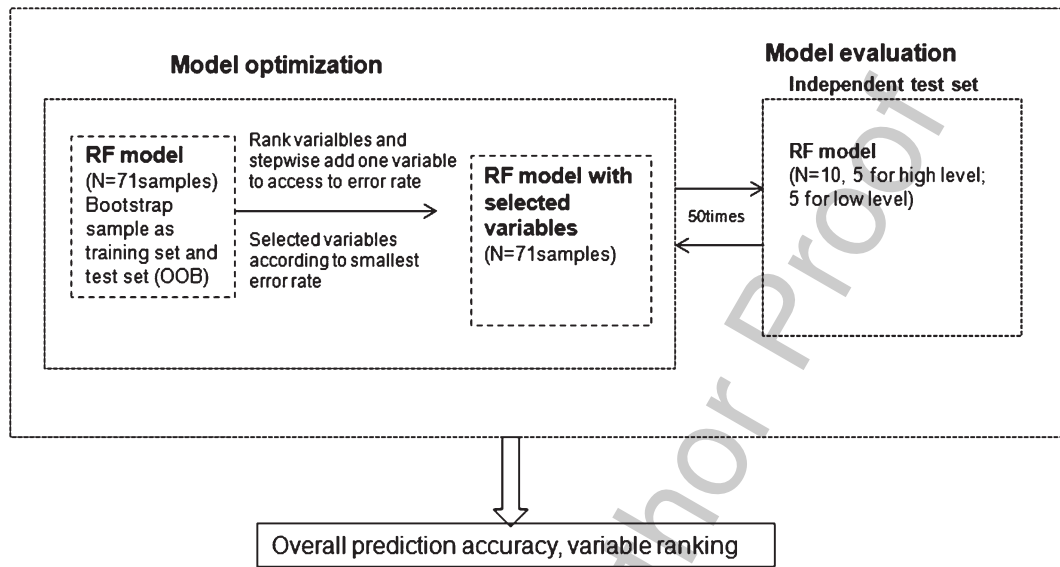


Fig. 2. Nested cross-validation machine learning schema to evaluate model and estimate prediction accuracy.

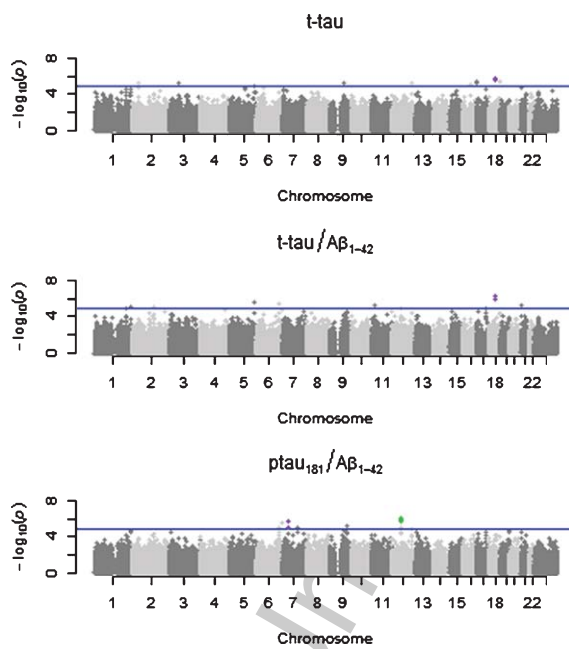


Fig. 3. Manhattan plots of GWAS of tau, tau/Aβ<sub>1-42</sub>, and ptau<sub>181</sub>/Aβ<sub>1-42</sub> as quantitative traits, respectively. The purple dots represent the candidate SNPs which are reached the threshold  $p < 5 \times 10^{-5}$  and at least two SNPs are in high LD ( $R^2 > 0.8$ ) as well. In “t-tau” subplot and “t-tau/Aβ<sub>1-42</sub>” subplot, rs1445093 and rs12327358 are represented by purple dots. In “ptau<sub>181</sub>/Aβ<sub>1-42</sub>” subplot, rs11975968 and rs17161127 are represented by purple dots; the top SNP rs1249963 from GWAS is represented by green dot.

188 filtered out if 1) minor allele frequency <5%; 2) missing  
189 genotype rate per SNP >95%; 3) missing genotype rate  
190 per individual >90%; and 4) Hardy-Weinberg Equilib-

rium  $p < 10^{-6}$ . In total, 514,932 SNPs were included  
191 in subsequent analysis. Genotype calls and QC was  
192 performed using PLINK (version 1.07) [28].  
193

A total of 514,932 SNPs and 177 subjects that passed  
194 QC were included in GWAS analysis.  
195

#### Genome-wide association analysis

We selected CSF biomarkers levels of t-tau, p-tau<sub>181</sub>,  
197 and the two ratios t-tau/Aβ<sub>1-42</sub> and p-tau<sub>181</sub>/Aβ<sub>1-42</sub>  
198 as quantitative traits (endophenotypes) for GWAS.  
199 CSF t-tau, p-tau<sub>181</sub> concentrations, and the two ratios  
200 t-tau/Aβ<sub>1-42</sub> and p-tau<sub>181</sub>/Aβ<sub>1-42</sub> were all observed to  
201 be approximately normally distributed after log<sub>2</sub> trans-  
202 formation.  
203

The main effect of SNPs was assessed on  
204 log<sub>2</sub>-transformed t-tau, p-tau<sub>181</sub>, and two ratios of  
205 log<sub>2</sub>-transformed t-tau/Aβ<sub>1-42</sub> and p-tau<sub>181</sub>/Aβ<sub>1-42</sub> as  
206 quantitative traits, separately. Linear models were fit-  
207 ted to identify associations dependent additively upon  
208 the minor allele, with adjustment for age, gender,  
209 and APOE4 status. Minor allele homozygotes were  
210 coded as 2, heterozygotes coded as 1, and major allele  
211 homozygotes were coded as 0. The four models based  
212 on four quantitative traits were designated as p-tau<sub>181</sub>  
213 model, t-tau model, p-tau<sub>181</sub>/Aβ<sub>1-42</sub> model, and t-tau/  
214 Aβ<sub>1-42</sub> model. For each trait, the linear regression  
215 model used to test for main effect of SNP was:

$$Y = \mu + \beta_1 * \text{SNP} + \beta_2 * \text{conversion} + \beta_3 * \text{AGE} + \beta_4 * \text{GENDER} + \beta_5 * \text{APOE4} + \epsilon$$

191  
192  
193  
194  
195

196

197  
198  
199  
200  
201  
202  
203

204  
205  
206  
207  
208  
209  
210  
211  
212  
213  
214  
215  
216  
217  
218

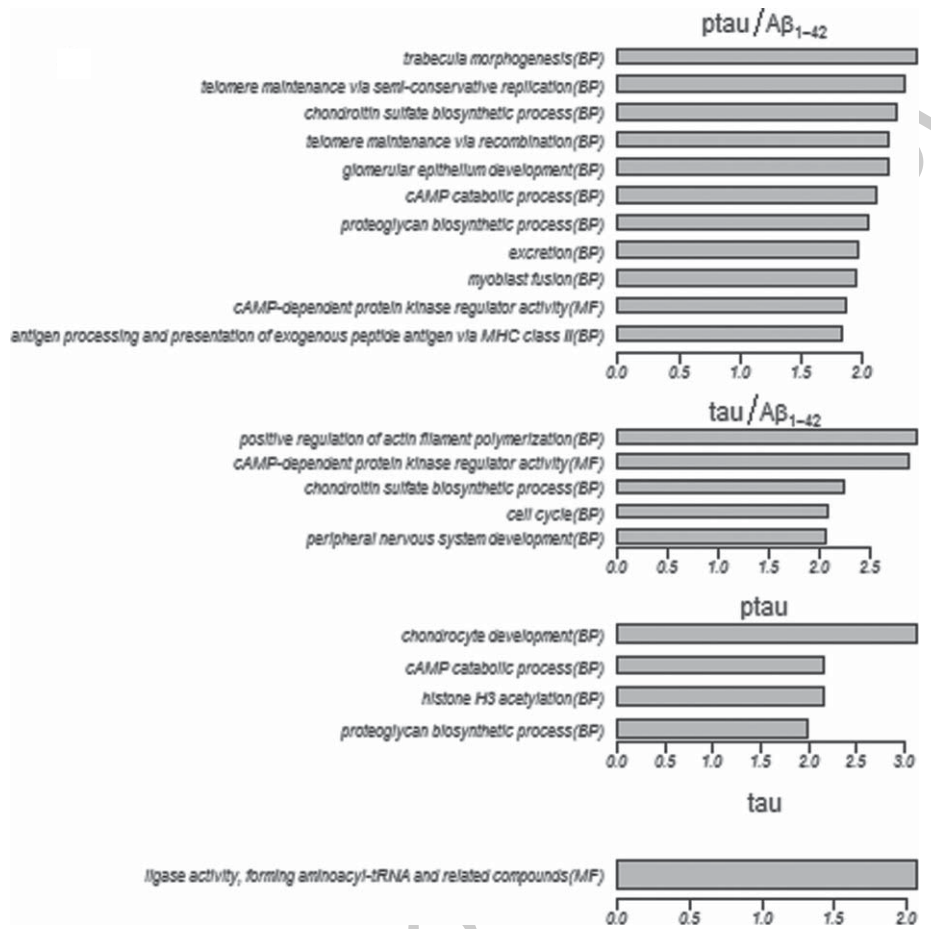


Fig. 4A. Enriched Gene Ontology terms for p-tau<sub>181</sub>. x-axis represents  $-\log_{10}(p\text{-value})$ .

219 The false discovery rate (FDR) for reported candi- 237  
 220 date SNPs were calculated using Benjamini and 238  
 221 Hochberg’s method [29]. 239

222 *Pathway and network analysis* 240

223 SNPs from the four GWAS analyses p-tau<sub>181</sub>, 241  
 224 p-tau<sub>181</sub>/Aβ<sub>1-42</sub> ratio, t-tau, and t-tau/Aβ<sub>1-42</sub> were 242  
 225 assigned to genes from the NCBI build 36, using 243  
 226 ProxyGeneLD which facilitates the conversion of 244  
 227 genome-wide genetic marker lists to representative 245  
 228 gene lists [30]. The two major features of this software 246  
 229 are assigning gene-based significance by accounting 247  
 230 for high linkage disequilibrium (LD) structure and cor- 248  
 231 recting the *p*-value according to marker density due 249  
 232 to the gene size. By consideration of high LD struc- 250  
 233 ture (user-specified *r*<sup>2</sup>) the software iteratively groups 251  
 234 SNPs into clusters. Cluster estimation uses LD infor- 252  
 235 mation to allow for associated markers beyond gene 253  
 236 windows and reduces false positive hits by accounting 254  
 255  
 256

237 for interdependence of SNPs. Thus, the most sig- 238  
 239 nificant marker assigned to a specific gene can in 239  
 240 turn reside outside of the specified gene boundaries. 240  
 241 Two user-specified parameters in software included 241  
 242 gene-boundary windows and the LD threshold, which 242  
 243 parameters we defined as 1 kb upstream of transcrip- 243  
 244 tion initiation sites to the end of the 3’ UTR of the 244  
 245 longest known splice form and *r*<sup>2</sup> > 0.8 for LD thresh- 245  
 246 old, respectively. 246

247 In order to characterize the functional role of top 247  
 248 genes in the list, and to identify significant pathway- 248  
 249 related SNPs for further predictive models, the top 249  
 250 three percent genes in each of the four gene lists con- 250  
 251 verted from the four GWAS SNPs lists were used in 251  
 252 pathway enrichment analysis with the public database 252  
 253 Gene Ontology (GO) and the Ingenuity® pathway anal- 253  
 254 ysis. The hypergeometric test and right-tailed Fisher’s 254  
 255 Exact test to find over-represented pathways were 255  
 256 applied to the output from GO and IPA, respectively. 256  
 Due to the acyclic GO structure, hypergeometric tests

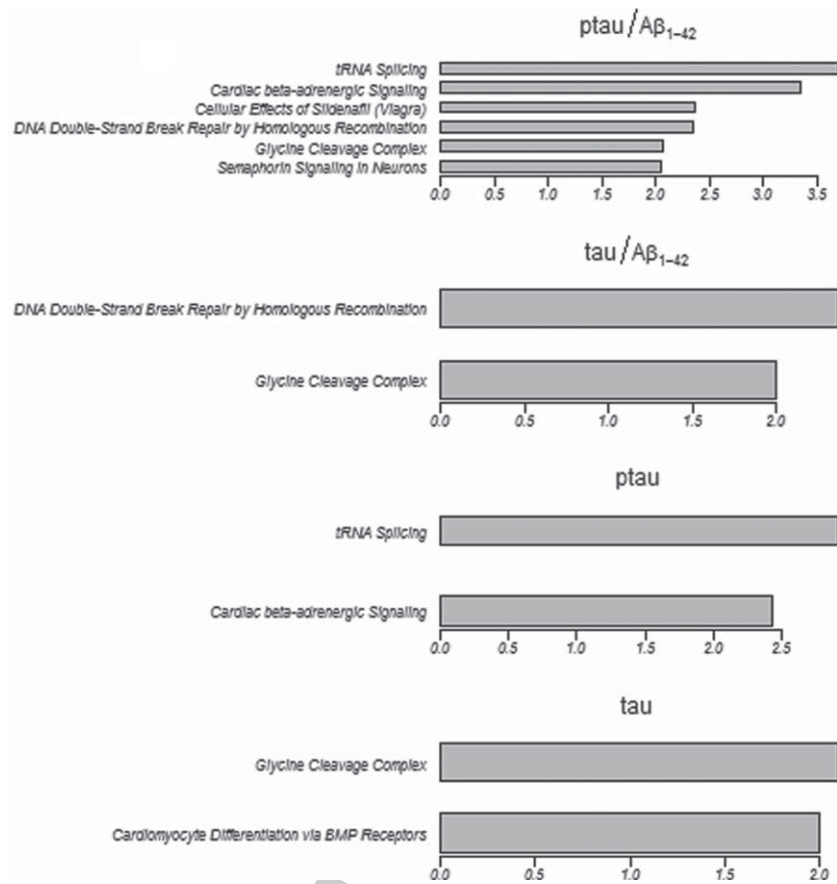


Fig. 4B. Significant canonical pathways from Ingenuity pathway analysis for p-tau<sub>181</sub> (A), p-tau<sub>181</sub>/A $\beta$ <sub>1-42</sub> ratio (B), t-tau (C), and t-tau/A $\beta$ <sub>1-42</sub> (D), respectively. x-axis represents  $-\log_{10}(p\text{-value})$ .

257 were performed with consideration for the GO structure,  
 258 such that tests were first performed for those terms  
 259 with no child terms. Before testing the terms whose  
 260 children had already been tested, all genes annotated  
 261 as significant children from the parent's gene list were  
 262 removed. This was continued until all terms had been  
 263 tested. The analysis was restricted to gene sets contain-  
 264 ing 10–200 genes since small pathways can exhibit  
 265 spurious phenotype associations due to large single  
 266 locus effects, and large pathways are more likely to  
 267 exhibit association by chance alone [22]. Significant  
 268 pathways were selected with  $p$  value  $\leq 0.01$ . We note  
 269 that ProxyGeneLD as used for conversion of SNPs  
 270 to genes treated the high LD block as a single signal  
 271 and chooses the  $p$  value of the best single marker  
 272 (lowest  $p$  value in LD block) in that LD block for  
 273 pre-adjustment significance level, which means that  
 274 the same marker may be assigned to a number of  
 275 genes in a high LD block and thus have the potential  
 276 to inflate pathway enrichment analysis. To avoid

277 this, we manually checked the significant pathway  
 278 results from the enrichment analysis. If a significant  
 279 pathway included several genes in a LD block, only  
 280 one gene was selected at random and the enrichment  
 281 analysis run again to test if the pathway was still sig-  
 282 nificant. A protein–protein interaction network was  
 283 constructed based on Ingenuity Knowledge Base using  
 284 IPAs defined algorithm [31].

#### Receiver operating characteristic curve analysis 285

286 In order to define cut-off points for subse-  
 287 quent binary classification from identified pathways,  
 288 receiver-operator characteristics (ROC) curves of the  
 289 MCI-con versus the MCI-stable group were plotted  
 290 by varying a cutoff from the baseline of t-tau and  
 291 p-tau<sub>181</sub> levels and the two ratios p-tau<sub>181</sub>/A $\beta$ <sub>1-42</sub>  
 292 and t-tau/A $\beta$ <sub>1-42</sub>. AUCs under the ROC curves, sen-  
 293 sitivities, specificities, and optimal thresholds were  
 294 calculated using the pROC package (version 1.5.4) in

the R software environment (version 3.0.0). The optimal threshold point was calculated using the Youden index method [32].

### Random Forest multivariate modeling

Random Forest (RF) modeling was applied to develop a predictive model for discrimination between low and high levels of p-tau<sub>181</sub>/Aβ<sub>1-42</sub> ratio, and to identify an associated biomarker panel consisting of a small number of predictors (SNPs). The SNPs were encoded as 0, 1, and 2, by minor allele count, when used as predictors in the RF model. To jointly evaluate the prediction performance and optimize RF parameters, a nested (double) cross-validation strategy was applied (Fig. 2); the samples were randomly divided into one training set (71 samples) used in the innermost cycle for parameter optimization and one test set (10 samples) used in the outermost cycle for prediction performance assessment. This process was repeated for 50 random partitions of the samples into training and test sets. Within the inner cycle, a RF model was trained, consisting of 1000 trees. A variable importance (VI score), Mean Decrease Accuracy, was calculated for all variables, and variables were ranked in descending order by VI score. Then, new models were constructed sequentially by stepwise addition of variables, one-at-a-time, and prediction error rates were evaluated. An RF model was optimized, with minimum number of variables (SNPs) and smallest prediction error rate, using the cross-validation training set in each inner cross-validation round. For each outer cross-validation round the samples in the independent test set were classified into low and high level of p-tau<sub>181</sub>/Aβ<sub>1-42</sub> ratio to assess prediction performance. The final prediction accuracy was calculated as the percentage of correctly classified samples across the 50 outer cross-validation rounds. The average of VI scores was calculated for each variable across the 50 iterations using training sets.

For selection of the most important variables, an overall VI score was calculated using the full set of samples. The correlation between overall VI score and average VI score from 50 iterations was calculated using Spearman's rank correlation test. Analysis was performed with the Random Forest package (version 4.6–7) in the R software environment. In order to validate the statistical significance of predictive performance of AUC from ROC analysis based on the small set of selected predictors, RF models were fitted to the same number of randomly selected SNPs/predictors from GWAS as in the obtained model using a boot-

strap approach. This procedure was repeated 100 times in order to obtain AUC values. The empirical *p* value of the AUC was then estimated as the proportion of sampled AUC values where AUC is greater or equal to the observed AUC value.

### High performance computing

GWAS, cross-validation, and bootstrap validation for RF models used the High Performance Computing (HPC) cluster resource at AstraZeneca, Mölndal, Sweden. The HPC consists of Dell M1000E blade centers, 176 nodes with two six-core Xeon processors, with 2–8GB of memory per core. The cluster contains 2,112 cores in total, all connected with Infiniband QDR for node inter-communication and storage access.

## RESULTS

### Demographic characteristics and CSF biomarkers of patients with MCI in ADNI

From the ADNI1-cohort, 177 MCI subjects with 48 months follow-up time and with a useable CSF sample at baseline were included in the analysis, 81 of these converted to AD and 96 were stable after to 48 months follow-up (Table 1). APOE ε4 allele status was significantly associated with MCI to AD conversion according to the one-sided Fisher's exact test ( $p=0.02313$ ).

Median and mean  $\pm$  SD values ( $\log_2$  transformed) for p-tau<sub>181</sub>, t-tau, and the two ratios of t-tau/Aβ<sub>1-42</sub> and p-tau<sub>181</sub>/Aβ<sub>1-42</sub> at baseline from the selected MCI-stable and MCI-con group in ADNI are summarized in Table 2. The CSF levels at baseline of p-tau<sub>181</sub> and the p-tau<sub>181</sub>/Aβ<sub>1-42</sub> ratio were significantly increased in the MCI-con group as compared with MCI-stable group, respectively (for p-tau<sub>181</sub>:  $p=0.01$ ; for p-tau<sub>181</sub>/Aβ<sub>1-42</sub>:  $p=0.006$ ), but not for t-tau or t-tau/Aβ<sub>1-42</sub> ( $p=0.21$ ;  $p=0.097$ ).

Table 1  
Demographic characteristics of MCI subjects who provided a cerebrospinal fluid sample at baseline visit and with 48 months follow-up time in ADNI cohort

	male/female	median AGE at baseline (range)	APOE ε4 carrier
MCI-stable ( $n=96$ )	66/30	75(55–89)	45 (47%)
MCI-converter ( $n=81$ )	52/29	75(55–89)	51 (63%)



Table 2  
Cerebrospinal fluid biomarker concentration and ratios for selected MCI subjects at baseline

	ptau181	ptau <sub>181</sub> /Aβ <sub>1-42</sub>	tau	tau/Aβ <sub>1-42</sub>
MCI-stable				
median	23.5	0.15	74.60	0.50
mean ± SD	30.3 ± 18.3	0.21 ± 0.17	94.79 ± 63.03	0.65 ± 0.59
MCI-con				
median	36.25	0.26	94.16	0.68
mean ± SD	37.02 ± 15.82	0.27 ± 0.15	106.70 ± 46.87	0.79 ± 0.48

380 *GWAS of CSF biomarkers t-tau, p-tau<sub>181</sub> and the*  
381 *two ratios of p-tau<sub>181</sub>/Aβ<sub>1-42</sub> and t-tau/Aβ<sub>1-42</sub>*

382 In order to perform pathway-based analysis and  
383 select significant pathway-related SNPs for down-  
384 stream analysis, GWAS analysis was performed as  
385 described above. After quality control, 514,932 SNPs  
386 were individually fitted in linear regression mod-  
387 els with covariate adjustment for age, gender, and  
388 APOE ε4 allele status to evaluate the association  
389 of SNPs with p-tau<sub>181</sub> concentration, t-tau concen-  
390 tration, p-tau<sub>181</sub>/Aβ<sub>1-42</sub> ratio, and t-tau/Aβ<sub>1-42</sub> ratio,  
391 respectively. After calculation of genomic inflation fac-  
392 tors [33] (p-tau<sub>181</sub> λ = 1.007, p-tau<sub>181</sub>/Aβ<sub>1-42</sub> λ = 1.012,  
393 t-tau λ = 1.005, t-tau/Aβ<sub>1-42</sub> λ = 1.012), no inflation was  
394 observed, which indicated that population stratification  
395 alone was unlikely to account for the GWAS results.

396 Top-ranked (*p* value < 10<sup>-5</sup>) candidate SNPs associ-  
397 ated with CSF biomarkers in the context of conversion  
398 from MCI to AD for the models t-tau, t-tau/Aβ<sub>1-42</sub>,  
399 p-tau<sub>181</sub>/Aβ<sub>1-42</sub>, and p-tau<sub>181</sub> are listed in Table 3.  
400 SNPs rs1445093 and rs12327358, which are in high  
401 LD (*r*<sup>2</sup> = 0.97), were associated with t-tau/Aβ<sub>1-42</sub> ratio,  
402 with *p* values of 2.80 × 10<sup>-7</sup> and 5.76 × 10<sup>-7</sup>, respec-  
403 tively (Fig. 3, purple dots in “t-tau/Aβ<sub>1-42</sub>” subplot).  
404 These two SNPs were also associated with t-tau with *p*  
405 value 3.73 × 10<sup>-7</sup> and 6.34 × 10<sup>-7</sup> (Fig. 3, purple dots  
406 in “t-tau” subplot). SNPs rs1445093 and rs12327358  
407 are located in an intergenic region on chromosome  
408 18 and are located circa 95kb and 90kb upstream,  
409 respectively, of the gene coding the Netrin recep-  
410 tor DCC (DCC). From the p-tau<sub>181</sub>/Aβ<sub>1-42</sub> model,  
411 we observed that rs1249963 was associated with p-  
412 tau<sub>181</sub>/Aβ<sub>1-42</sub> with *p* value 8.85 × 10<sup>-7</sup> (Fig. 3, green  
413 dot in the “ptau<sub>181</sub>/Aβ<sub>1-42</sub>” subplot). rs1249963 is  
414 located in an intergenic region on chromosome 12 and  
415 7kb upstream of *PPP1R1A* (protein phosphatase 1,  
416 regulatory (inhibitor) subunit 1A). SNPs rs11975968  
417 (*p*-value: 1.53 × 10<sup>-6</sup>) and rs17161127 (*p*-value:  
418 7.71 × 10<sup>-6</sup>), are located in the first intron of phos-  
419 phodiesterase 1C, calmodulin-dependent (PDE1C) on

chromosome 7, and are in high LD (*r*<sup>2</sup> > 0.8) (Fig. 3,  
purple dots in “ptau<sub>181</sub>/Aβ<sub>1-42</sub>” subplot).

#### Pathway analysis

In order to characterize the functional role of SNPs  
and the corresponding genes and gene products asso-  
ciated with the four traits (p-tau<sub>181</sub>, t-tau, and two  
ratios p-tau<sub>181</sub>/Aβ<sub>1-42</sub> and t-tau/Aβ<sub>1-42</sub>), respectively,  
we performed a marker-to-gene conversion and anal-  
yzed the top 3% of genes for pathway enrichment  
analysis for each trait. This procedure yielded four  
lists of genes associated with each trait ranked by  
significance. From GO analysis, we identified sev-  
eral statistically significantly enriched (*p* value < 0.01)  
GO terms in the “biological processes” and “molec-  
ular function” that were associated with the top 3%  
of genes from the p-tau<sub>181</sub>, p-tau<sub>181</sub>/Aβ<sub>1-42</sub>, t-tau, and  
t-tau/Aβ<sub>1-42</sub> models, respectively (Fig. 4A). Shared  
enriched GO terms between the p-tau<sub>181</sub> and p-  
tau<sub>181</sub>/Aβ<sub>1-42</sub> traits were “cAMP catabolism process”  
and “proteoglycan biosynthesis”. Shared enriched GO  
terms between p-tau<sub>181</sub>/Aβ<sub>1-42</sub> and t-tau/Aβ<sub>1-42</sub> traits  
were “cAMP-dependent protein kinase regulation” and  
“chondroitin sulphate biosynthesis”. We also observed  
that pathways for “positive regulation of actin filament  
polymerization” (CDC42EP2, FMN1, RHOA, RAC1,  
CCL21, and CCL24) and “peripheral nervous system  
development” (FOXD2, PMP22, ISL2, TBCE, and  
RUNX1) significantly associated with t-tau/Aβ<sub>1-42</sub>.

Significantly associated canonical pathways (*p*  
value < 0.01) were similarly identified using Ingenu-  
ity Pathway Analysis (IPA) (Fig. 4B). The “Glycine  
cleavage complex” pathway was associated to the p-  
tau<sub>181</sub>/Aβ<sub>1-42</sub>, t-tau and t-tau/Aβ<sub>1-42</sub> models. GCSH  
(glycine cleavage system H protein) and AMT  
(aminomethyltransferase) were associated with the  
“Glycine cleavage complex” pathway (energy produc-  
tion, lipid metabolism). The “cardiac beta-adrenergic  
signalling” pathway was shared by p-tau<sub>181</sub> and p-  
tau<sub>181</sub>/Aβ<sub>1-42</sub> traits. A number of genes, PDE1B,  
PDE1C, PDE3B, PDE6D, and PDE8A, encoding  
cyclic nucleotide phosphodiesterases (PDEs) were  
found to be associated with this pathway.

#### Predictive models for pathway-derived SNPs/genes associated with p-tau<sub>181</sub>/Aβ<sub>1-42</sub> in APOE4-negative patients

In order to identify genetic markers predictive  
of CSF biomarkers that are known in turn to pre-  
dict MCI to AD conversion [15, 16], we performed



Table 3  
SNPs ( $p$  value  $< 1 \times 10^{-5}$ ) selected from GWAS for each trait. In each model, \*represents SNPs in high LD (LD  $> 0.8$ )

SNPs name	$P$ value	FDR	chromosome	Gene
SNPs from GWAS of t-tau				
rs1445093*	3.73E-07	0.16	18	–
rs12327358*	6.34E-07	0.16	18	–
rs4239351	1.29E-06	0.22	18	–
rs11078506	4.95E-06	0.58	17	–
rs11124499	6.13E-06	0.58	2	–
rs3885648	7.47E-06	0.58	3	TMEM132C
rs1466134	8.01E-06	0.58	16	GPR56
SNPs from GWAS of t-tau/ Aβ <sub>1-42</sub>				
rs1445093*	2.80E-07	0.14	18	–
rs12327358*	5.76E-07	0.15	18	–
rs7131051	3.08E-06	0.40	11	NAV2
rs2824765	3.29E-06	0.40	21	TMPRSS15
rs4869001	3.90E-06	0.40	5	–
rs12130076	6.91E-06	0.55	1	–
rs1249963	7.81E-06	0.55	12	–
rs4577811	9.16E-06	0.55	6	PLEKHG1
SNPs from GWAS of p-tau <sub>181</sub> /Aβ <sub>1-42</sub>				
rs1249963	8.85E-07	0.37	12	–
rs11975968*	1.53E-06	0.37	7	PDE1C
rs10945919	2.13E-06	0.37	6	–
rs2157673	4.32E-06	0.51	9	–
rs4895598	7.31E-06	0.51	6	–
rs17161127*	7.71E-06	0.51	7	PDE1C
rs1716355	7.90E-06	0.51	12	GLYCAM1
rs1143960	8.47E-06	0.51	12	PPP1RIA
rs2107284	8.91E-06	0.51	7	–
SNPs from GWAS of p-tau <sub>181</sub> .				
rs11975968	2.99E-06	0.55	7	PDE1C
rs12809589	4.45E-06	0.55	12	TMEM132C
rs11795346	4.75E-06	0.55	9	ZNF169
rs10945919	6.92E-06	0.55	6	–
rs11059821	7.87E-06	0.55	12	TMEM132C
rs11795331	8.13E-06	0.55	9	ZNF169

468 ROC analysis for CSF biomarkers with stratification  
 469 by APOE  $\epsilon$ 4 allele status. Results showed that all  
 470 four CSF biomarker classifiers performed best in the  
 471 APOE4-negative subgroup (Supplementary Figure 1  
 472 and Supplementary Table 1). The optimized cut-offs  
 473 for p-tau<sub>181</sub>, ptau<sub>181</sub>/Aβ<sub>1-42</sub>, t-tau, and t-tau/Aβ<sub>1-42</sub>  
 474 to predict MCI to AD conversion for APOE4-negative  
 475 subject were 20 pg/ml, 70 pg/ml, 0.13 and 0.25,  
 476 respectively. The p-tau<sub>181</sub>/Aβ<sub>1-42</sub> ratio was selected  
 477 as response variable (binned response variable for two  
 478 categories of high/low) in further predictive models  
 479 considering that of both sensitivity and specificity were  
 480 greater than 60%, thus higher in comparison with other  
 481 CSF biomarkers (Supplementary Table 2).

482 From GO and IPA enrichment analysis, 51 non-  
 483 redundant genes were identified as related to 49 SNPs  
 484 (Supplementary Table 3) and associated with GO terms  
 485 or IPA canonical pathways in turn significantly associ-  
 486 ated to the ptau/Aβ<sub>1-42</sub> ratio trait, as described above.  
 487 Having identified pathway-associated genes/SNPs in  
 488 the GWAS analysis, and having identified optimal

489 cutoff points for binary classifiers (low/high level of  
 490 ptau<sub>181</sub>/Aβ<sub>1-42</sub> ratio), we performed predictive mod-  
 491 eling in the APOE4-negative group patients using  
 492 these 49 SNPs as predictors and low/high level of  
 493 ptau<sub>181</sub>/Aβ<sub>1-42</sub> ratio with respect to the optimized cut-  
 494 off as the response variable.

495 An RF model was constructed for prediction of high  
 496 or low ratio of p-tau<sub>181</sub>/Aβ<sub>1-42</sub> in the APOE4-negative  
 497 group. Cross-validation was applied to evaluate predic-  
 498 tion performance of the RF model, and the average  
 499 sensitivity was estimated to 66% and specificity to  
 500 70%. The AUC value was 0.74 from ROC anal-  
 501 ysis ( $p$  value = 0.01) (Fig. 5). The correlation of  
 502 variable rankings according to VI score using all  
 503 samples and average VI score from 50 iteration of  
 504 cross-validation was highly significant (Spearman's  
 505 rank correlation test,  $p$ -value  $< 2.2e^{-16}$ ). Five SNPs  
 506 rs6766238, rs1143960, rs1249963, rs11975968, and  
 507 rs4836493 were selected as important variables/SNPs,  
 508 these SNPs were ranked as top five in both in the rank-  
 509 ing list based on overall VI score using all samples and

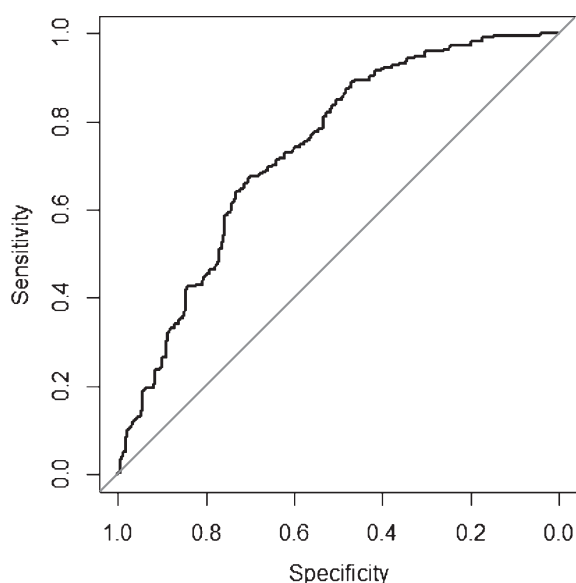


Fig. 5. Receiver operating characteristic analysis for prediction the baseline level of p-tau<sub>181</sub>/A $\beta$ <sub>1-42</sub> ratio (high/low) using SNP data based on RF model in APOE4-negative subjects. The straight diagonal line illustrates prediction by pure chance (AUC 0.5), and the curved line describes the predictions using the RF models when varying the cut-off values (AUC 0.74,  $p$  value = 0.01).

510 in the list based on the average VI score from cross-  
 511 validation. The corresponding candidate genes of these  
 512 SNPs are listed in Table 4 together with the observed  
 513 protein expression in human brain from the Human  
 514 Protein Atlas (HPA) [34]. We note that SNPs assigned  
 515 to a specific gene can reside outside of specified gene  
 516 boundaries due to consideration of LD structure as  
 517 discussed above, and that LD blocks may contain  
 518 more than one gene. Distribution of p-tau<sub>181</sub>/A $\beta$ <sub>1-42</sub>  
 519 ratio by genotype for the five SNPs is shown in  
 520 Fig. 6.

521 In order to characterize the functional role of the  
 522 identified genes, potential interconnections among the  
 523 seven candidate protein products was explored and  
 524 a functional network was built upon the Ingenuity  
 525 pathway knowledge base (Fig. 7). From the protein-  
 526 protein interaction network, we could observe that  
 527 several candidate gene products indirectly connected  
 528 with Ca<sup>2+</sup>, which might indicate that the progression  
 529 of AD pathology is correlated with changes of intracel-  
 530 lular Ca<sup>2+</sup> concentration. Most of these genes encode  
 531 proteins that demonstrate moderate to strong protein  
 532 expression in cerebral cortex, lateral ventricle, hip-  
 533 pocampus, or cerebellum, suggesting that these genes  
 534 might indeed play an important role in CNS function  
 535 and in AD pathology.

Table 4  
 RNA/protein expression level in CNS from Human Protein Atlas  
 database (HPA) for identified candidate genes

Representative SNP	Gene	CNS(brain) from HPA
rs1143960	PDE1B	Strong in cerebral cortex, lateral ventricle, and cerebellum
rs11975968	PDE1C	Strong in cerebral cortex
rs1249963	PPP1R1A	Strong in cerebral cortex, hippocampus, lateral ventricle, and cerebellum
rs6766238	AMT	Strong in cerebral cortex, cerebellum and moderate in hippocampus
rs6766238	RHOA	Moderate in cerebral cortex, hippocampus and cerebellum
rs6766238	DAG1	Moderate expression in cerebral cortex
rs4836493	CHSY3	Moderate in cerebral cortex

## DISCUSSION

536 In this study, we developed and applied an inte-  
 537 grated analysis approach that combined GWAS,  
 538 pathway enrichment analysis, and predictive model-  
 539 ing to identify genetic factors predictive of baseline  
 540 CSF biomarkers, which may thus ultimately be pre-  
 541 dictive of AD progression from MCI to AD. For  
 542 single SNP analysis, we applied a conventional GWAS  
 543 approach to identify top-ranked SNPs associated with  
 544 CSF biomarkers t-tau, p-tau<sub>181</sub>, t-tau/A $\beta$ <sub>1-42</sub>, and  
 545 p-tau<sub>181</sub>/A $\beta$ <sub>1-42</sub>. In addition, we also performed path-  
 546 way enrichment analysis in order to get biological  
 547 insight and take into account potential joint genetic  
 548 effects. Through these analyses, we could prioritize  
 549 a limited number of candidate SNPs for building  
 550 the predictive models. We have been able to iden-  
 551 tify a panel of five SNPs, rs6766238, rs11975968,  
 552 rs1143960, rs1249963, and rs4836493, that are pre-  
 553 dictively informative for baseline p-tau<sub>181</sub>/A $\beta$ <sub>1-42</sub> ratio  
 554 (high/low, cutoff 0.13) with 66% sensitivity and 70%  
 555 specificity in APOE4-negative subjects. It is notable  
 556 that the optimal cutoff used for the predictive model  
 557 (0.13) is close to the median ratio for p-tau<sub>181</sub>/A $\beta$ <sub>1-42</sub>  
 558 from the MCI APOE4-negative carrier group (0.12),  
 559 suggesting that the genetic test could have a signifi-  
 560 cant clinical impact after further validation. rs6766238  
 561 is representative for an LD block containing protein  
 562 coding genes for *RHOA*, *AMT*, and *DAG1*. It has  
 563 been shown that *RHOA* protein abundance is decreased  
 564 in the AD brain hippocampus, and *RHOA* colocal-  
 565 ized with hyperphosphorylated tau in Pick's disease,  
 566 a neurodegenerative disorder characterized by hyper-  
 567 phosphorylated tau accumulation [35]. It has been  
 568

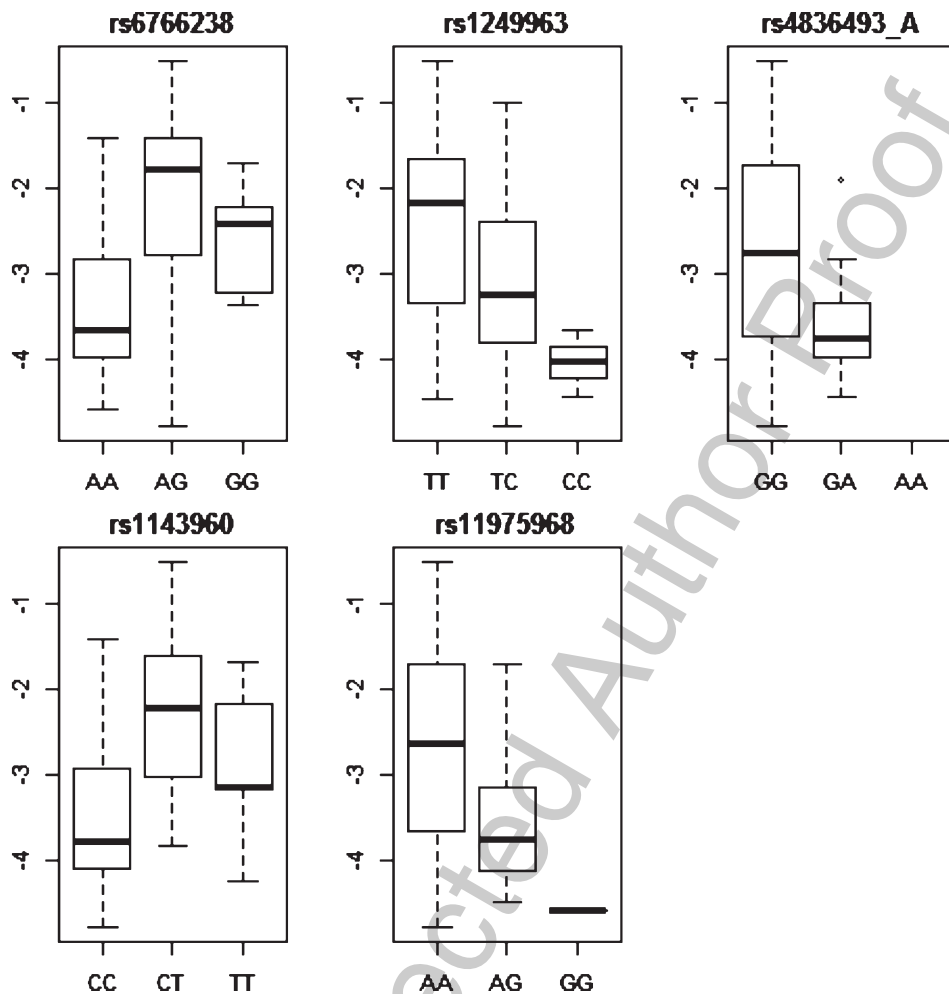
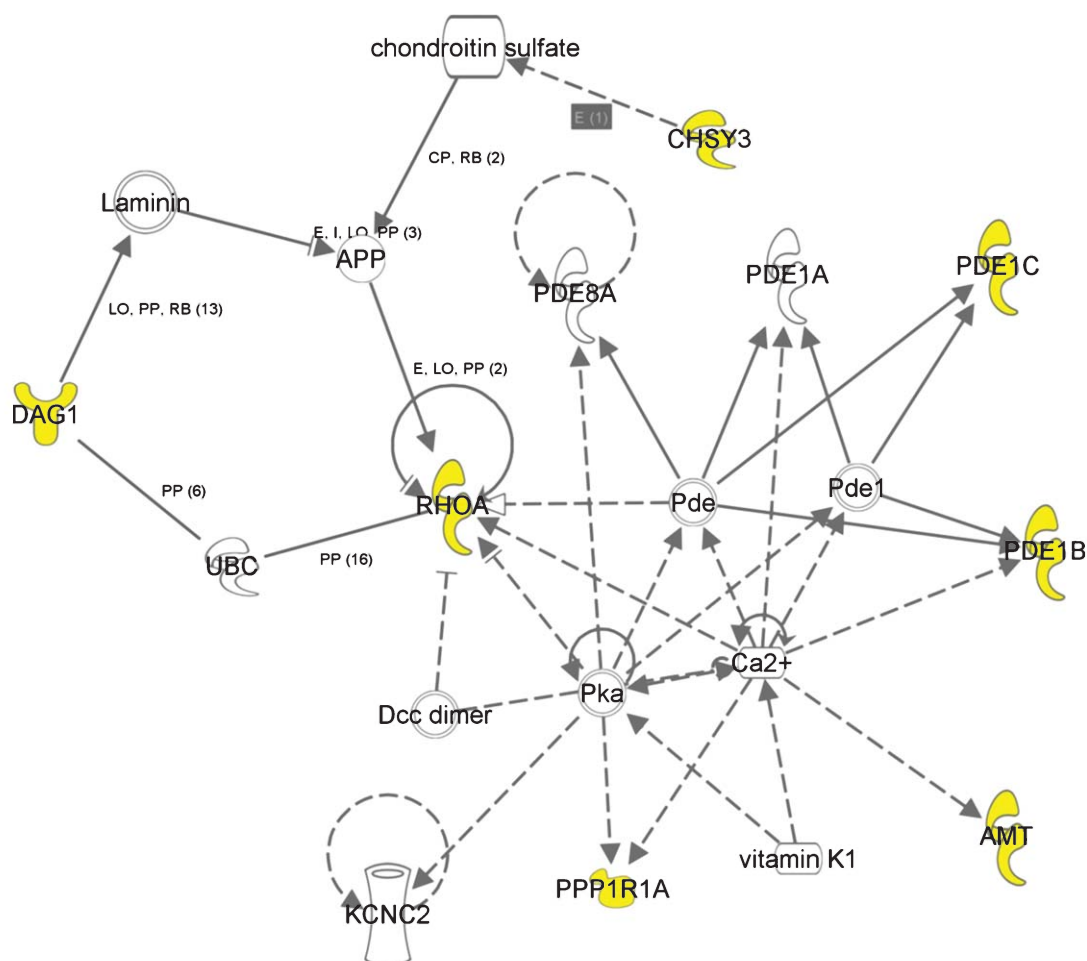


Fig. 6. Boxplots of ratio of ptau/A $\beta$ <sub>1-42</sub> (log2 transformed) grouped by genotype for five candidate SNPs in APOE4-negative subjects. Each boxplot is in the order homozygous major allele, heterozygous, homozygous minor allele at each SNP.

569 shown that *DAG1* encoding protein alpha-dystroglycan  
 570 exhibits higher levels in AD CSF as compared with  
 571 normal subjects [36]. rs1143960 is representative for  
 572 *PDE1B* (phosphodiesterase 1B, Calcium/calmodulin-  
 573 dependent). rs1249963 is located in intergenic region  
 574 of genome, but it is representative for *PPP1R1A* due  
 575 to LD structure. rs11975968 is located in the intronic  
 576 portion of *PDE1C* (phosphodiesterase 1C, calmodulin-  
 577 dependent). rs4836493 is located in the intron region of  
 578 gene *CHSY3* (chondroitin sulfate synthase 3). *PDE1B*  
 579 and *PDE1C* are members of the *PDE1* family. *PDE1*  
 580 family is activated by the binding of calmodulin in  
 581 the presence of Ca<sup>2+</sup> and is capable of acting on  
 582 both cAMP and cGMP. *PDE1* has several isoforms;  
 583 *PDE1B* is expressed in brain and mainly in dopamin-  
 584 ergic regions [37]. *PDE1C* is highly expressed in the  
 585 heart, but also found in the CNS [38, 39]. *PPP1R1A* is

involved in long-term potentiation of synapses (LTP).  
 It has been shown that deficiency of this gene in mouse  
 causes different degrees of impairment of LTP, indicat-  
 ing that these genes play a role in synaptic plasticity  
 [40]. Bossers et al. showed that using Braak staging for  
 neurofibrillary changes as an objective indicator of pro-  
 gression of AD, *PPP1R1A* expression was decreased  
 in early Braak stages, followed by an increase in  
 expression in later stages [41]. In summary, the genes  
 identified in the model have face validity as potential  
 modulators of calcium regulation and hence control  
 of phosphorylation in neuronal signal transduction,  
 and thus may contribute to the modulation of AD  
 progression by interaction with pathways downstream  
 from A $\beta$ . This study also suggests that pharmaco-  
 logical intervention at these targets may have future  
 utility.

586  
 587  
 588  
 589  
 590  
 591  
 592  
 593  
 594  
 595  
 596  
 597  
 598  
 599  
 600  
 601  
 602



© 2000-2014 QIAGEN. All rights reserved.

Fig. 7. Protein-protein interaction network from the Ingenuity pathway knowledge base. Protein products of selected candidate genes are highlighted in yellow. A solid line indicates the known experiment-confirmed direct interaction and a dashed line indicates indirect interaction.

603 In pathway enrichment analysis, proteoglycan  
 604 biosynthesis was significantly associated with the p-  
 605 tau<sub>181</sub> and p-tau<sub>181</sub>/A $\beta$ <sub>1-42</sub> traits. It is known that  
 606 proteoglycans are associated with amyloid deposi-  
 607 tion and it has been reported that heparin sulphate  
 608 proteoglycans are involved in the pathogenesis of  
 609 AD [42]. Furthermore, it has been shown that chon-  
 610 droitin sulphate-containing proteoglycan is found in  
 611 senile plaques of human AD tissue [43]. *NCAN*  
 612 (neurocan), *CHSY3* (chondroitin sulfate synthase 3),  
 613 and *CHST7* (carbohydrate (N-acetylglucosamine 6-O)  
 614 sulfotransferase 7) were associated with the “proteo-  
 615 glycan biosynthetic process” pathway. Interestingly,  
 616 the pathway of telomere maintenance via semi-  
 617 conservative replication was significantly associated

with p-tau<sub>181</sub>/A $\beta$ <sub>1-42</sub>. There is some evidence linking  
 shortened telomeres to AD [44, 45].

In this study, we investigated CSF biomarkers as  
 predictors of conversion from MCI to AD, stratified  
 by the presence of the APOE  $\epsilon$ 4 allele. We observed  
 that CSF biomarkers in APOE4-negative subjects out-  
 performed APOE4-positive subjects in discriminating  
 MCI-con and MCI-stable. Our observation is sup-  
 ported by data recently published by Apostolova et al.  
 who showed that using CSF biomarker as a classifier  
 to predict conversion from MCI to AD performed bet-  
 ter in APOE4-negative subjects than APOE4-positive  
 subjects [25]. One explanation based on our analysis  
 is that there are significant differences in baseline  
 levels of CSF biomarkers between MCI-con and MCI-  
 stable

618  
 619  
 620  
 621  
 622  
 623  
 624  
 625  
 626  
 627  
 628  
 629  
 630  
 631  
 632

633 in the APOE4-negative group, while there is no sig- 685  
634 nificant difference between MCI-con and MCI-stable 686  
635 in APOE4-positive group. We also observed that base- 687  
636 line levels of CSF t-tau, p-tau<sub>181</sub>, t-tau/Aβ<sub>1-42</sub>, and 688  
637 p-tau<sub>181</sub>/Aβ<sub>1-42</sub> were greater in the APOE4-positive 689  
638 group as compared with the APOE4-negative group. 690  
639 High CSF t-tau or p-tau<sub>181</sub> and low CSF Aβ<sub>1-42</sub> are 691  
640 linked to the tau and Aβ pathologies of AD and APOE 692  
641 ε4 is a strong risk factor for AD development. 693

642 One of the main aims of this study was to identify 694  
643 candidate genetic markers to predict CSF biomarkers 695  
644 in the context of progression from MCI to AD using an 696  
645 integrated analytics approach rather than single-locus 697  
646 based GWAS approach. Our results provided AUC esti- 698  
647 mated to 0.74 ( $p$  value = 0.01), suggesting that the RF 699  
648 model based on the candidate biomarker panel pro- 700  
649 vides a means to discriminate between high and low 701  
650 ratio of p-tau<sub>181</sub>/Aβ<sub>1-42</sub> in APOE4-negative subjects. 702  
651 genes implicated by the identified predictive markers 703  
652 show moderate to strong protein expression in cerebral 704  
653 cortex, lateral ventricle, hippocampus or cerebellum, 705  
654 indicating that these genes might be correlated to CNS 706  
655 function. It is clear that additional work is required 707  
656 to replicate and validate the findings. Replication in 708  
657 additional cohorts and additional analysis to determine 709  
658 likely underlying functional variants to investigate the 710  
659 clinical, histological, and functional cell biological 711  
660 consequences of those changes are all warranted as 712  
661 objectives of further studies.

662 A limitation of the current study is the small sam-  
663 ple size of MCI subjects for GWAS analysis and  
664 present lack of an independent cohort for valida-  
665 tion. We were limited to 177 subjects in ADNI1 that  
666 had CSF biomarkers data and so could be included  
667 into this model approach at the time of our study.  
668 Taking into account the known heterogeneity of the  
669 aMCI clinical diagnosis and the small effect size  
670 the common genetic variants, we will have low  
671 power to detect genome-wide significant associa-  
672 tions ( $p < 5 \times 10^{-7}$ ) of individual variants in the GWAS  
673 analysis using conventional Bonferroni multiple test  
674 correction. However, Bonferroni's method is overly  
675 conservative because the independence assumption  
676 does not hold due to the LD structure among SNPs.  
677 Therefore, the top-ranked GWAS SNPs were primarily  
678 used to identify significant pathways through pathway  
679 analysis. The reported top-ranked SNPs in this study  
680 should be considered as potential candidates for repli-  
681 cation and validation in future studies. Future studies  
682 with potential for replication include ADNI-GO and  
683 ADNI-2, where early MCI subjects are being recruited  
684 and all patients in ADNI-2 undergo lumbar punctures

for CSF data collection, which will increase sample  
size and statistical power. Moreover, the World Wide  
ADNI (WW-ADNI) consortium is actively developing  
broader collaboration efforts to contribute in this com-  
munity. Large datasets from WW-ADNI are likely to  
be become available in the future and could provide  
more replication samples.

Diagnostic criteria in the field of AD remain in  
development, and even advanced clinical AD remains a  
probable diagnosis that is not confirmable antemortem.  
Emerging guidelines suggest that the addition of one  
or two biomarkers to the clinical status would add  
value [4], however, no genetic markers are yet val-  
idated in this context. Moreover, current biomarker  
methodologies are invasive and expensive (primarily  
lumbar puncture and PET imaging). Much attention is  
thus focused on the identification of less invasive alter-  
natives. The identification of genetic signatures that  
can complement or even ultimately replace biochemi-  
cal biomarkers in a diagnostic or prognostic scenario  
is thus a potential future avenue. Despite the limita-  
tion of sample size for this study as we discussed,  
the final SNP model is designed to demonstrate that  
a genetic signature can predict level of baseline bio-  
chemical biomarkers, which in turn are predictive of  
future conversion of MCI to AD. Hence, the marker  
panel identified in this study may have utility in screen-  
ing and/or stratification for future treatments.

## ACKNOWLEDGMENTS

The authors wish to acknowledge valuable discus-  
sions with Mun-Gwan Hong at SciLifeLab, School of  
Biotechnology, KTH-Royal Institute of Technology,  
Stockholm and Andreas Loong in High Performance  
Computing, AstraZeneca, Mölndal, Sweden.

Data collection and sharing for this project was  
funded by the Alzheimer's Disease Neuroimaging Ini-  
tiative (ADNI) (National Institutes of Health Grant  
U01 AG024904) and DOD ADNI (Department of  
Defense award number W81XWH-12-2-0012). ADNI  
is funded by the National Institute on Aging, the  
National Institute of Biomedical Imaging and Bio-  
engineering, and through generous contributions from  
the following: Alzheimer's Association; Alzheimer's  
Drug Discovery Foundation; BioClinica, Inc.; Biogen  
Idec Inc.; Bristol-Myers Squibb Company; Eisai Inc.;  
Elan Pharmaceuticals, Inc.; Eli Lilly and Company;  
F. Hoffmann-La Roche Ltd and its affiliated com-  
pany Genentech, Inc.; GE Healthcare; Innogenetics,  
N.V.; IXICO Ltd.; Janssen Alzheimer Immunotherapy

Research & Development, LLC.; Johnson & Johnson Pharmaceutical Research & Development LLC.; Medpace, Inc.; Merck & Co., Inc.; Meso Scale Diagnostics, LLC.; NeuroRx Research; Novartis Pharmaceuticals Corporation; Pfizer Inc.; Piramal Imaging; Servier; Synarc Inc.; and Takeda Pharmaceutical Company. The Canadian Institutes of Health Research is providing funds to support ADNI clinical sites in Canada. Private sector contributions are facilitated by the Foundation for the National Institutes of Health (www.fnih.org). The grantee organization is the Northern California Institute for Research and Education, and the study is Rev December 5, 2013 coordinated by the Alzheimer's Disease Cooperative Study at the University of California, San Diego. ADNI data are disseminated by the Laboratory for Neuro Imaging at the University of Southern California.

Authors' disclosures available online (<http://j-alz.com/manuscript-disclosures/14-2118r2>).

## SUPPLEMENTARY MATERIAL

The supplementary material is available in the electronic version of this article: <http://dx.doi.org/10.3233/JAD-142118>.

## REFERENCES

- [1] Prince M, Bryce R, Albanese E, Wimo A, Ribeiro W, Ferri CP (2013) The global prevalence of dementia: A systematic review and metaanalysis. *Alzheimers Dement* **9**, 63-75.e2.
- [2] Petersen RC, Smith GE, Waring SC, Ivnik RJ, Tangalos EG, Kokmen E (1999) Mild cognitive impairment: Clinical characterization and outcome. *Arch Neurol* **56**, 303-308.
- [3] Manly JJ, Tang MX, Schupf N, Stern Y, Vonsattel JP, Mayeux R (2008) Frequency and course of mild cognitive impairment in a multiethnic community. *Ann Neurol* **63**, 494-506.
- [4] Cummings JL, Dubois B, Molinuevo JL, Scheltens P (2013) International Work Group criteria for the diagnosis of Alzheimer disease. *Med Clin North Am* **97**, 363-368.
- [5] Dubois B, Epelbaum S, Santos A, Di Stefano F, Julian A, Michon A, Sarazin M, Hampel H (2013) Alzheimer disease: From biomarkers to diagnosis. *Rev Neurol (Paris)* **169**, 744-751.
- [6] Dubois B, Feldman HH, Jacova C, Hampel H, Molinuevo JL, Blennow K, DeKosky ST, Gauthier S, Selkoe D, Bateman R, Cappa S, Crutch S, Engelborghs S, Frisoni GB, Fox NC, Galasko D, Habert MO, Jicha GA, Nordberg A, Pasquier F, Rabinovici G, Robert P, Rowe C, Salloway S, Sarazin M, Epelbaum S, de Souza LC, Vellas B, Visser PJ, Schneider L, Stern Y, Scheltens P, Cummings JL (2014) Advancing research diagnostic criteria for Alzheimer's disease: The IWG-2 criteria. *Lancet Neurol* **13**, 614-629.
- [7] Cohen AD, Klunk WE (2014) Early detection of Alzheimer's disease using PiB and FDG PET. *Neurobiol Dis* **72PA** 117-122.
- [8] Herholz K, Westwood S, Haense C, Dunn G (2011) Evaluation of a calibrated (18)F-FDG PET score as a biomarker for progression in Alzheimer disease and mild cognitive impairment. *J Nucl Med* **52**, 1218-1226.
- [9] Salas-Gonzalez D, Gorritz JM, Ramirez J, Illan IA, Lopez M, Segovia F, Chaves R, Padilla P, Puntinet CG (2010) Feature selection using factor analysis for Alzheimer's diagnosis using 18F-FDG PET images. *Med Phys* **37**, 6084-6095.
- [10] Brown RK, Bohnen NI, Wong KK, Minoshima S, Frey KA (2014) Brain PET in suspected dementia: Patterns of altered FDG metabolism. *Radiographics* **34**, 684-701.
- [11] Cui Y, Liu B, Luo S, Zhen X, Fan M, Liu T, Zhu W, Park M, Jiang T, Jin JS, Alzheimer's Disease Neuroimaging Initiative (2011) Identification of conversion from mild cognitive impairment to Alzheimer's disease using multivariate predictors. *PLoS One* **6**, e21896.
- [12] De Riva V, Galloni E, Marcon M, Di Dionisio L, Deluca C, Meligrana L, Bolner A, Perini F (2014) Analysis of combined CSF biomarkers in AD diagnosis. *Clin Lab* **60**, 629-634.
- [13] Vemuri P, Wiste HJ, Weigand SD, Shaw LM, Trojanowski JQ, Weiner MW, Knopman DS, Petersen RC, Jack CR jr, Alzheimer's Disease Neuroimaging Initiative (2009) MRI and CSF biomarkers in normal, MCI, and AD subjects: Predicting future clinical change. *Neurology* **73**, 294-301.
- [14] Samtani MN, Raghavan N, Shi Y, Novak G, Farnum M, Lobanov V, Schultz T, Yang E, DiBernardo A, Narayan VA, Alzheimer's Disease Neuroimaging Initiative (2013) Disease progression model in subjects with mild cognitive impairment from the Alzheimer's disease neuroimaging initiative: CSF biomarkers predict population subtypes. *Br J Clin Pharmacol* **75**, 146-161.
- [15] Shaw LM, Vanderstichele H, Knopik-Czajka M, Clark CM, Aisen PS, Petersen RC, Blennow K, Soares H, Simon A, Lewczuk P, Dean R, Siemers E, Potter W, Lee VM, Trojanowski JQ, Alzheimer's Disease Neuroimaging Initiative (2009) Cerebrospinal fluid biomarker signature in Alzheimer's disease neuroimaging initiative subjects. *Ann Neurol* **65**, 403-413.
- [16] Hansson O, Zetterberg H, Buchhave P, Londos E, Blennow K, Minthon L (2006) Association between CSF biomarkers and incipient Alzheimer's disease in patients with mild cognitive impairment: A follow-up study. *Lancet Neurol* **5**, 228-234.
- [17] Davatzikos C, Bhatt P, Shaw LM, Batmanghelich KN, Trojanowski JQ (2011) Prediction of MCI to AD conversion, via MRI, CSF biomarkers, and pattern classification. *Neurobiol Aging* **32**, 2322.e19-2322.e27.
- [18] De Meyer G, Shapiro F, Vanderstichele H, Vanmechelen E, Engelborghs S, De Deyn PP, Coart E, Hansson O, Minthon L, Zetterberg H, Blennow K, Shaw L, Trojanowski JQ, Alzheimer's Disease Neuroimaging Initiative (2010) Diagnosis-independent Alzheimer disease biomarker signature in cognitively normal elderly people. *Arch Neurol* **67**, 949-956.
- [19] Bertram L, Tanzi RE (2012) The genetics of Alzheimer's disease. *Prog Mol Biol Transl Sci* **107**, 79-100.
- [20] Sorbi S, Nacmias B, Forleo P, Latorraca S, Gobbi I, Bracco L, Piacentini S, Amaducci L (1994) ApoE allele frequencies in Italian sporadic and familial Alzheimer's disease. *Neurosci Lett* **177**, 100-102.
- [21] Strittmatter WJ, Weisgraber KH, Huang DY, Dong LM, Salvesen GS, Pericak-Vance M, Schmechel D, Saunders AM, Goldgaber D, Roses AD (1993) Binding of human apolipoprotein E to synthetic amyloid beta peptide: Isoform-specific effects and implications for late-onset Alzheimer disease. *Proc Natl Acad Sci U S A* **90**, 8098-8102.
- [22] Cruchaga C, Karch CM, Jin SC, Benitez BA, Cai Y, Guerreiro R, Harari O, Norton J, Budde J, Bertelsen S, Jeng AT, Cooper

- B, Skorupa T, Carrell D, Levitch D, Hsu S, Choi J, Ryten M, UK Brain Expression Consortium, Hardy J, Ryten M, Trabzuni D, Weale ME, Ramasamy A, Smith C, Sassi C, Bras J, Gibbs JR, Hernandez DG, Lupton MK, Powell J, Forabosco P, Ridge PG, Corcoran CD, Tschanz JT, Norton MC, Munger RG, Schmutz C, Leary M, Demirci FY, Bamne MN, Wang X, Lopez OL, Ganguli M, Medway C, Turton J, Lord J, Braae A, Barber I, Brown K, UK Alzheimer's Research Consortium, Passmore P, Craig D, Johnston J, McGuinness B, Todd S, Heun R, Kolsch H, Kehoe PG, Hooper NM, Vardy ER, Mann DM, Pickering-Brown S, Brown K, Kalsheker N, Lowe J, Morgan K, David Smith A, Wilcock G, Warden D, Holmes C, Pastor P, Lorenzo-Betancor O, Brkanac Z, Scott E, Topol E, Morgan K, Rogava E, Singleton AB, Hardy J, Kamboh MI, St George-Hyslop P, Cairns N, Morris JC, Kauwe JS, Goate AM (2014) Rare coding variants in the phospholipase D3 gene confer risk for Alzheimer's disease. *Nature* **505**, 550-554.
- [23] Naj AC, Jun G, Beecham GW, Wang LS, Vardarajan BN, Buros J, Gallins PJ, Buxbaum JD, Jarvik GP, Crane PK, Larson EB, Bird TD, Boeve BF, Graff-Radford NR, De Jager PL, Evans D, Schneider JA, Carrasquillo MM, Ertekin-Taner N, Younkin SG, Cruchaga C, Kauwe JS, Nowotny P, Kramer P, Hardy J, Huentelman MJ, Myers AJ, Barmada MM, Demirci FY, Baldwin CT, Green RC, Rogava E, St George-Hyslop P, Arnold SE, Barber R, Beach T, Bigio EH, Bowen JD, Boxer A, Burke JR, Cairns NJ, Carlson CS, Carney RM, Carroll SL, Chui HC, Clark DG, Comeveaux J, Cotman CW, Cummings JL, DeCarli C, DeKosky ST, Diaz-Arrastia R, Dick M, Dickson DW, Ellis WG, Faber KM, Fallon KB, Farlow MR, Ferris S, Frosch MP, Galasko DR, Ganguli M, Gearing M, Geschwind DH, Ghetti B, Gilbert JR, Gilman S, Giordani B, Glass JD, Growdon JH, Hamilton RL, Harrell LE, Head E, Honig LS, Hulette CM, Hyman BT, Jicha GA, Jin LW, Johnson N, Karlawish J, Karydas A, Kaye JA, Kim R, Koo EH, Kowall NW, Lah JJ, Levey AI, Lieberman AP, Lopez OL, Mack WJ, Marson DC, Martiniuk F, Mash DC, Masliah E, McCormick WC, McCurry SM, McDavid AN, McKee AC, Mesulam M, Miller BL, Miller CA, Miller JW, Parisi JE, Perl DP, Peskind E, Petersen RC, Poon WW, Quinn JF, Rajbhandary RA, Raskind M, Reisberg B, Ringman JM, Roberson ED, Rosenberg RN, Sano M, Schneider LS, Seeley W, Shelanski ML, Slifer MA, Smith CD, Sonnen JA, Spina S, Stern RA, Tanzi RE, Trojanowski JQ, Troncoso JC, Van Deerlin VM, Vinters HV, Vonsattel JP, Weintraub S, Welsh-Bohmer KA, Williamson J, Woltjer RL, Cantwell LB, Dombroski BA, Beekly D, Lunetta KL, Martin ER, Kamboh MI, Saykin AJ, Reiman EM, Bennett DA, Morris JC, Montine TJ, Goate AM, Blacker D, Tsuang DW, Hakonarson H, Kukull WA, Foroud TM, Haines JL, Mayeux R, Pericak-Vance MA, Farrer LA, Schellenberg GD (2011) Common variants at MS4A4/MS4A6E, CD2AP, CD33 and EPHA1 are associated with late-onset Alzheimer's disease. *Nat Genet* **43**, 436-441.
- [24] Peterson D, Munger C, Crowley J, Corcoran C, Cruchaga C, Goate AM, Norton MC, Green RC, Munger RG, Breitner JC, Welsh-Bohmer KA, Lyketsos C, Tschanz J, Kauwe JS, Alzheimer's Disease Neuroimaging Initiative (2014) Variants in PPP3R1 and MAPT are associated with more rapid functional decline in Alzheimer's disease: The Cache County Dementia Progression Study. *Alzheimers Dement* **10**, 366-371.
- [25] Apostolova LG, Hwang KS, Kohannim O, Avila D, Elashoff D, Jack CR Jr, Shaw L, Trojanowski JQ, Weiner MW, Thompson PM, Alzheimer's Disease Neuroimaging Initiative (2014) ApoE4 effects on automated diagnostic classifiers for mild cognitive impairment and Alzheimer's disease. *Neuroimage Clin* **4**, 461-472.
- [26] Breiman L (2001) Random Forests. *Machine Learn* **45**, 5-32.
- [27] Saykin AJ, Shen L, Foroud TM, Potkin SG, Swaminathan S, Kim S, Risacher SL, Nho K, Huentelman MJ, Craig DW, Thompson PM, Stein JL, Moore JH, Farrer LA, Green RC, Bertram L, Jack CR Jr, Weiner MW, Alzheimer's Disease Neuroimaging Initiative (2010) Alzheimer's Disease Neuroimaging Initiative biomarkers as quantitative phenotypes: Genetics core aims, progress, and plans. *Alzheimers Dement* **6**, 265-273.
- [28] Purcell S, Neale B, Todd-Brown K, Thomas L, Ferreira MA, Bender D, Maller J, Sklar P, de Bakker PI, Daly MJ, Sham PC (2007) PLINK: A tool set for whole-genome association and population-based linkage analyses. *Am J Hum Genet* **81**, 559-575.
- [29] Hochberg YBY (1990) More powerful procedures for multiple significance testing. *Stat Med* **9**, 811-818.
- [30] Hong MG, Pawitan Y, Magnusson PK, Prince JA (2009) Strategies and issues in the detection of pathway enrichment in genome-wide association studies. *Hum Genet* **126**, 289-301.
- [31] Ingenuity pathway analysis. Network Generation Algorithm. (October 29, 2005).
- [32] Youden WJ (1950) Index for rating diagnostic tests. *Cancer* **3**, 32-35.
- [33] Bacanu SA, Devlin B, Roeder K (2000) The power of genomic control. *Am J Hum Genet* **66**, 1933-1944.
- [34] The Human Protein Atlas, <http://www.proteinatlas.org/>
- [35] Huesa G, Baltrons MA, Gomez-Ramos P, Moran A, Garcia A, Hidalgo J, Frances S, Santpere G, Ferrer I, Galea E (2010) Altered distribution of RhoA in Alzheimer's disease and AbetaPP overexpressing mice. *J Alzheimers Dis* **19**, 37-56.
- [36] Yin GN, Lee HW, Cho JY, Suk K (2009) Neuronal penta-oxin receptor in cerebrospinal fluid as a potential biomarker for neurodegenerative diseases. *Brain Res* **1265**, 158-170.
- [37] Medina AE (2011) Therapeutic utility of phosphodiesterase type I inhibitors in neurological conditions. *Front Neurosci* **5**, 21.
- [38] Lakics V, Karran EH, Boess FG (2010) Quantitative comparison of phosphodiesterase mRNA distribution in human brain and peripheral tissues. *Neuropharmacology* **59**, 367-374.
- [39] Menniti FS, Faraci WS, Schmidt CJ (2006) Phosphodiesterases in the CNS: Targets for drug development. *Nat Rev Drug Discov* **5**, 660-670.
- [40] Allen PB, Hvalby O, Jensen V, Errington ML, Ramsay M, Chaudhry FA, Bliss TV, Storm-Mathisen J, Morris RG, Andersen P, Greengard P (2000) Protein phosphatase-1 regulation in the induction of long-term potentiation: Heterogeneous molecular mechanisms. *J Neurosci* **20**, 3537-3543.
- [41] Bossers K, Wirz KT, Meerhoff GF, Essing AH, van Dongen JW, Houba P, Kruse CG, Verhaagen J, Swaab DF (2010) Concerted changes in transcripts in the prefrontal cortex precede neuropathology in Alzheimer's disease. *Brain* **133**, 3699-3723.
- [42] van Horsen J, Wesseling P, van den Heuvel LP, de Waal RM, Verbeek MM (2003) Heparan sulphate proteoglycans in Alzheimer's disease and amyloid-related disorders. *Lancet Neurol* **2**, 482-492.
- [43] Canning DR, McKeon RJ, DeWitt DA, Perry G, Wujek JR, Frederickson RC, Silver J (1993) beta-Amyloid of Alzheimer's disease induces reactive gliosis that inhibits axonal outgrowth. *Exp Neurol* **124**, 289-298.



- 983 [44] Hochstrasser T, Marksteiner J, Humpel C (2012) Telomere length is age-dependent and reduced in monocytes of Alzheimer patients. *Exp Gerontol* **47**, 160-163. 990
- 984 991
- 985 992
- 986 [45] Cai Z, Yan LJ, Ratka A (2013) Telomere shortening and Alzheimer's disease. *Neuromolecular Med* **15**, 25-48. 993
- 987 994
- 988 [46] Ferreira D, Rivero-Santana A, Perestelo-Perez L, Westman E, Wahlund LO, Sarria A, Serrano-Aguilar P (2014) Improving CSF biomarkers' performance for predicting progression from mild cognitive impairment to Alzheimer's disease by considering different confounding factors: A meta-analysis. *Front Aging Neurosci* **6**, 287. 995
- 989 996
- [47] Palmqvist S, Hertze J, Minthon L, Wattmo C, Zetterberg H, Blennow K, Londos E, Hansson O (2012) Comparison of brief cognitive tests and CSF biomarkers in predicting Alzheimer's disease in mild cognitive impairment: Six-year follow-up study. *PLoS One* **7**, e38639. 997

Uncorrected Author Proof